

# A Fully Conservative Ghost Fluid Method & Stiff Detonation Waves

Duc Nguyen  
Computer Science Department  
Stanford University  
Stanford, CA 94305

Frédéric Gibou  
Computer Science Department and Mathematics Department  
Stanford University  
Stanford, CA 94305

Ronald Fedkiw  
Computer Science Department  
Stanford University  
Stanford, CA 94305

We present a new, fully conservative version of the ghost fluid method applicable for tracking material interfaces, inert shocks, and both deflagration and detonation waves in as many as three spatial dimensions. The exact discrete conservation properties are most important when tracking inert shocks and detonation waves, so that is the focus of this paper. In particular, we address the inviscid reactive Euler equations in the context of stiff detonation waves on coarse grids. The main difficulty here arises when the time scales of the chemical reaction are significantly shorter than the time scales of the fluid dynamics leading to a stiff source term and nonphysical wave phenomena. We use the level set method to track the location of the detonation wave and the ghost fluid method to treat the discontinuous quantities across the inert shock portion of that wave. This leads to a sharp non-smearred shock profile alleviating the nonphysical wave phenomena.

## 1 - Introduction

In this paper, we address the numerical approximation of detonation waves in a shock-capturing framework. The main difficulties arise when the chemical reactions introduce time scales that are significantly shorter than the hydrodynamic time scales. Standard shock capturing algorithms smear out the front so that a few grid cells lie within the shock profile. The numerically smeared out temperature profile contains values that are artificially raised above the ignition temperature with the potential to trigger the chemical reaction too

early. When the reaction is fast, the gas can be completely burnt in the next time step shifting the discontinuity to the adjacent cell boundary leading to a nonphysical one-grid-cell per time step spurious wave. This phenomenon was first observed by Colella et al. [12].

Engquist and Sjögreen [13] addressed this issue by evaluating the reaction term a few grid cells ahead of the shock so that the chemical reaction is not triggered in the numerically smeared out shock profile. However, finding the temperature “in front” of the wave is not trivial especially in higher spatial dimensions. First,

one has to design a method that determines the location of the moving front *and* the direction in which it is moving. Then one has to choose temperature values ahead of the front exercising caution in regions of high curvature and near domain or phase boundaries. For more details on detonations, solid walls and curvature, see [4]. Instead of evaluating the temperature “in front” of the wave, Bao and Jin [5,6] proposed a direct treatment of the smeared out temperatures within the numerical shock profile. Their approach is based on the random choice method of Chorin [11] (and Glimm [18]). They use a classical modern shock capturing method followed by a projection step that projects the chemically non-equilibrium data into equilibrium according to the value of a uniformly distributed random ignition temperature. This method ensures that the statistical average yields the correct speed.

Even for stiff chemical reactions, the problem becomes solvable under high enough resolution. Eventually, once enough grid points are added, the entire smeared out shock profile passes over a grid cell before the chemical reaction gets started. That is, once the induction time is large compared to the time it takes the numerically smeared out shock profile to pass over a grid cell, the combustion zone correctly lags behind the inert shock and the difficulties with shock capturing cease to be relevant. This has led authors such as Bihari and Schwendeman [8] to propose methods that aim to locally resolve the detonation wave with a large number of adaptively placed grid cells. Their method is based on the multiresolution schemes of Harten [23]. While this approach works well in one spatial dimension, both the scheme design and the number of grid cells needed to resolve stiff chemical reactions makes multidimensional calculations less promising.

Since one cannot always resolve the detonation wave such that the chemical reaction zone separates from the inert shock profile, a robust approach for treating short induction times is desirable. A direct approach to alleviating difficulties associated with smeared out shock profiles is to remove the smearing altogether along the lines of front tracking methods [21,10,7,28,20,19,22]. Unfortunately, three-dimensional front tracking can be rather difficult to implement requiring complex smoothing operations, interface surgery, etc. (see e.g. [32]).

An alternative to three-dimensional front tracking is the ghost fluid method of Fedkiw et al. [15] which uses level sets and a Riemann problem capturing framework to obtain sharp non-smeared discontinuities in a shock-capturing framework that is simple to extend to even three spatial dimensions. In [16], the ghost fluid method was extended to treat inert shock waves (see also [3]). [16] also proposed a model for tracking sharp detonation and deflagration waves, although they used a simplified model for detonations that assumes a zero induction time and an infinite reaction speed so that all the heat release can be folded into the shock front. This is a valid approach when the grid does not resolve the fast time scale of the reaction and the small induction time. However, as the grid is resolved, the detonation wave should separate into an inert shock wave followed by a smooth reaction zone, and this simplified model cannot capture this behavior. In this paper, we extend their approach to allow for separate modeling of the shock wave and chemical reaction zone when the grid is relatively fine while still allowing stable and accurate calculations on coarse grids.

In the context of either front tracking or the ghost fluid method, removing numerical smearing is not enough to guarantee a robust numerical method. While this removes the chemical reaction zone from the shock itself, a

fast chemical reaction will still adversely affect the accuracy of the grid cell values in the post shock state. Since both the front tracking method and the ghost fluid method depend on the pre-shock and post-shock states to calculate the speed of the front, both methods will have difficulties computing the correct front speed. Thus, we design fully conservative version of the ghost fluid method applicable in as many as three spatial dimensions. Then we rely on exact discrete conservation of mass, momentum and energy to obtain valid wave speeds. Note that the individual species mass,  $\rho Y$ , is not conserved due to the presence of the source term, however, [17] extended the Lax-Wendroff Theorem [25] to show that one can obtain correct weak solutions without conserving this quantity.

## 2 - Equations

The basic equations for compressible flow with a one step irreversible chemical reaction are the reactive Euler equations. We consider these equations in two spatial dimensions but emphasize that the method is straightforward to extend to three spatial dimensions. This system of equations is written as

$$\begin{pmatrix} \rho \\ \rho u \\ \rho v \\ E \\ \rho Y \end{pmatrix}_t + \begin{pmatrix} \rho u \\ \rho u^2 + p \\ \rho uv \\ (E + p)u \\ \rho u Y \end{pmatrix}_x + \begin{pmatrix} \rho v \\ \rho uv \\ \rho v^2 + p \\ (E + p)v \\ \rho v Y \end{pmatrix}_y = \begin{pmatrix} 0 \\ 0 \\ 0 \\ 0 \\ S \end{pmatrix}$$

where  $t$  is time,  $(x, y)$  are the spatial coordinates,  $\rho$  is the density,  $\vec{V} = (u, v)$  are the velocities,  $E$  is the total energy per unit volume,  $p$  is the pressure, and  $Y$  is the mass fraction of unreacted fluid. The total energy is the sum of the internal energy and kinetic energy,  $E = \rho e + \rho(u^2 + v^2)/2$ , where  $e$  is the internal energy per unit mass. For simplicity,

we assume that both gases are ideal with the same specific heat ratio  $\gamma$  and that the internal energy of formation of the reacted gas is zero. Then, we can write  $p = (\gamma - 1)\rho(e - Ye_0)$ , with  $e_0$  the internal energy of formation of the unreacted gas. The temperature is given by  $T = p/(\rho R)$ , and the speed of sound is given by  $c = \sqrt{\gamma p/\rho}$ . For Arrhenius kinetics,  $S = -K\rho Y e^{-T_i/T}$  where  $T_i$  is the ignition temperature.

We use the level set method [27,26] to track the location of the inert shock front. Let  $\Phi$  be the signed distance function and define the unreacted fluid region by  $\Phi > 0$ , the reacted fluid region by  $\Phi < 0$ , and the front location by  $\Phi = 0$ . Then the front location is evolved according to

$$\Phi_t + \vec{W} \cdot \vec{\nabla} \Phi = 0 \quad (1)$$

where  $\vec{W} = D\vec{N}$  is the speed of the front and  $\vec{N} = \nabla \Phi / \|\nabla \Phi\|$  is the local unit normal. Here,  $D = D(\vec{U}^{(1)}, \vec{U}^{(2)})$  is the speed of the inert shock based on the pre-shock and post-shock states. For example, [16] used

$$D = \sqrt{\frac{\rho^{(1)}(V_N^{(1)})^2 + p^{(1)} - \rho^{(2)}(V_N^{(2)})^2 - p^{(2)}}{\rho^{(1)} - \rho^{(2)}}} \quad (2)$$

although more robust formulas for  $D$  can be obtained using Roe averages or by solving a Riemann problem. As  $\Phi$  is evolved in time according to equation (1), the new values of  $\Phi$  will not generally represent a signed distance function. Thus,  $\Phi$  is reinitialized to a signed distance function by solving

$$\Phi_\tau + \text{Sign}(\Phi_0)(\|\nabla \Phi\| - 1) = 0$$

for a few time steps in fictitious time  $\tau$ , see e.g. [31].

### 3 - The Ghost Fluid Method

The philosophy behind the ghost fluid method is to capture the correct boundary conditions at the interface while avoiding the traditional numerical smearing present in standard shock-capturing schemes. Fedkiw et al. [15] originally devised the ghost fluid method to alleviate numerical smearing and subsequent nonphysical oscillations at material interfaces (see also [14] and [2] for solid/fluid coupling). In this section, we address the variant of the method developed in [16] that allows one to track inert shocks.

The level set function is used to track the location of the inert shock and to determine whether a grid point is in the pre-shocked or post-shocked fluid (see section 2). Then, near the zero level set, the jump (boundary) conditions are captured by defining ghost cells on both sides of the shock front to represent the mass, momentum and energy of the real fluid from the other side of the inert shock front. In this fashion, both fluids are defined at every grid cell surrounding the shock front, and one can solve for each fluid independently using a standard shock-capturing scheme. Then, the level set function is evolved forward in time and the values of the real fluid are chosen according to the sign of the level set function. The values in the ghost cells are then discarded and the process is repeated.

The key to applying this method is to identify the continuous and discontinuous quantities to ensure that the appropriate jump (boundary) conditions are satisfied. The continuous variables are copied into the ghost cells in a node-by-node fashion (ensuring the continuity in these variables), while the discontinuous variables are extrapolated into the ghost cells from the other side of the interface in order to avoid the numerical dissipation errors intrinsic to standard shock-capturing schemes.

As in [16], the mass, momentum and energy fluxes in the moving reference frame (speed  $D$ ) should be continuous across any discontinuity. This leads to continuity of

$$\begin{aligned} F_\rho &= \rho(V_N - D) \\ F_{\rho V_N} &= \rho(V_N - D)^2 + p \\ F_E &= \left( \rho e + \frac{\rho(V_N - D)^2}{2} + p \right) (V_N - D) \end{aligned}$$

where  $V_N = \vec{V} \cdot \vec{N}$  is the velocity perpendicular to the discontinuity with local unit normal  $\vec{N}$  (easily computed using the level set function). In addition, as long as the discontinuity is not a contact discontinuity (i.e.  $D \neq V_N$ ), continuity of the two-dimensional tangential velocity can be expressed as continuity of

$$\vec{F}_{\rho V_T} = \vec{V} - V_N \vec{N}$$

which is expressed as a three-component vector for algorithmic convenience. For inert shocks,

$$F_{\rho Y} = \rho Y (V_N - D)$$

is continuous as well.

The ghost fluid is defined in a node-by-node fashion by solving the system of equations:  $F_\rho^G = F_\rho^R$ ,  $F_{\rho V_N}^G = F_{\rho V_N}^R$ ,  $F_E^G = F_E^R$ ,  $\vec{F}_{\rho V_T}^G = \vec{F}_{\rho V_T}^R$ ,  $F_{\rho Y}^G = F_{\rho Y}^R$  at each grid point. Here, the superscripts “ $R$ ” and “ $G$ ” stand for the real fluid values and the ghost fluid values respectively. At each grid node, if the speed of the discontinuity,  $D$ , is given, the real fluid values (with the “ $R$ ” superscript) can simply be evaluated. Then using the equation of state,  $p = (\gamma - 1)\rho(e - Ye_0)$ , one can write a quadratic equation for  $V_N^G - D$  equal to

$$\frac{\gamma F_{\rho V_N}^R}{(\gamma+1)F_{\rho}^R} \pm \sqrt{\left(\frac{\gamma F_{\rho V_N}^R}{(\gamma+1)F_{\rho}^R}\right)^2 - \frac{2(\gamma-1)}{(\gamma+1)}\left(\frac{F_E^R}{F_{\rho}^R} - Y^R e_o\right)}$$

where the “ $\pm$ ” sign is chosen as follows. When constructing a post-shocked ghost fluid,  $D$  should be subsonic relative to the flow (i.e.  $|V_N^G - D| < c^G$ ), and when constructing a pre-shocked ghost fluid,  $D$  should be supersonic relative to the flow (i.e.  $|V_N^G - D| > c^G$ ). Therefore, the “ $\pm$ ” sign should be chosen to give the minimum value of  $|V_N^G - D|$  when constructing a post-shocked ghost fluid and the maximum value of  $|V_N^G - D|$  when constructing a pre-shocked ghost fluid.

Once  $V_N^G$  is determined, finding  $\rho^G$ ,  $p^G$  and  $e^G$  is straightforward noting that the mass fraction of unreacted material is continuous across the shock, i.e.  $Y^G = Y^R$ . The velocity in the ghost cells,  $\vec{V}^G$ , is obtained by combining the normal velocity of the ghost fluid with the tangential velocity of the real fluid through the equation

$$\vec{V}^G = V_N^G \vec{N} + (\vec{V}^R - V_N^R \vec{N})$$

where  $V_N^R = \vec{V}^R \cdot \vec{N}$  is the normal velocity of the real fluid. For more details, see [16].

In summary, once  $D$  is defined at each grid node, the ghost cell values are defined in a node-by-node fashion as outlined above. In order to find  $D$  at each grid node, we extrapolate the pre-shock state  $\bar{U}^{(1)}$  across the interface into the post-shock region and extrapolate the post-shock state  $\bar{U}^{(2)}$  across the

interface into the pre-shock region. Then  $\bar{U}^{(1)}$  and  $\bar{U}^{(2)}$  are both defined at every grid point in a band near the interface, and the relation for  $D = D(\bar{U}^{(1)}, \bar{U}^{(2)})$  can be evaluated in a node-by-node fashion. The multidimensional extrapolation is carried out in the direction normal to the interface according to the equation  $I_r \pm \vec{N} \cdot \nabla I = 0$  where  $I$  represents a variable to be extrapolated and the “ $\pm$ ” sign is chosen to extrapolate either in the normal direction or opposite that direction. We solve this equation using a “fast marching” type method as explained in [1].

#### 4 - A Fully Conservative Ghost Fluid Method

Although the ghost fluid method produces highly accurate solutions without the characteristic numerical smearing of the discontinuity observed in standard shock capturing schemes, the method suffers from a lack of exact discrete conservation. For contact discontinuities where the interface speed is derived from the continuous linearly degenerate fluid velocity, this is not a serious issue. However for shocks (and detonations), the lack of exact discrete conservation raises concerns in light of the Lax-Wendroff theorem. Both the front tracking and ghost fluid methods circumvent potential difficulties associated with the lack of conservation by solving either exact or approximate Riemann problems to obtain the correct shock speed, see e.g. [16]. This requires valid pre-shock and post-shock states and thus works well for shocks surrounded by piecewise constant data such as those encountered in various test problems. However, in more difficult problems, such as stiff detonation waves, the pre-shock and post-shock states can be adversely affected by stiff chemistry, geometry and multidimensional effects such as curvature. Thus, we present a

new, fully conservative version of the ghost fluid method.

Two problems must be addressed in order to make the ghost fluid method fully conservative. First, the conservation errors need to be identified and measured, and then these errors need to be corrected. Identifying these errors in the context of a multidimensional application of the ghost fluid method might seem daunting. Not only are multi-valued fluxes used at some cell boundaries, but ghost cell values are converted into real grid cell values as the level set passes over them. This has led some authors, e.g. [22], to consider full space-time differencing, which is complicated in one spatial dimension and quite difficult to implement in multiple spatial dimensions. We instead propose a simpler alternative. For the sake of exposition, we present the method in two spatial dimensions emphasizing that it is straightforward to extend to three spatial dimensions as well.

Let  $U$  represent a quantity we wish to conserve, i.e. mass, momentum or energy. At the beginning of a time step, we determine the total amount of  $U$  in each cell as  $U^{old}$  based on the grid cell values  $U^n$ , e.g. in cells away from the interface  $U^{old} = U^n \Delta x \Delta y$  (we take some liberty with the conversion from point values to cell average values here valid to second order accuracy, but our method can be formally extended to cell averages as well). Near the interface, the zero level set cuts through the cell and we have  $U^{old} = (fU_1^n + (1-f)U_2^n) \Delta x \Delta y$  where  $0 \leq f \leq 1$  is the fraction of the cell occupied by  $U_1^n$  and  $1-f$  is the fraction of the cell occupied by  $U_2^n$ . A direct advantage of the ghost fluid method is that valid values of both  $U_1^n$  and  $U_2^n$  (i.e. values for both fluids) are stored at the cell centers of the grid cells near the interface. Also,  $f$  is easily calculated by applying a contouring algorithm to the zero

level set, e.g. see [9] for the version we use in two spatial dimensions.

After taking a time step (an Euler step or a full Runge-Kutta cycle), we reapply the algorithm above to calculate  $U^{new}$ . For a fully conservative algorithm  $U^{new}$  should be identical to  $U^{old} - \Delta t \Delta y (F^R - F^L) - \Delta t \Delta x (F^T - F^B)$  where  $F^R$ ,  $F^L$ ,  $F^T$  and  $F^B$  are the fluxes on the four sides of the cell. Moreover, these fluxes should be identical across cell boundaries, e.g.  $F_{i,j}^R = F_{i+1,j}^L$ . To evaluate the conservation errors, we take a cell-centric approach. At each cell center, the ghost fluid method updates the cell center value in time choosing all four fluxes from one fluid or the other. So, in each cell we *define* the four fluxes ( $F^R$ ,  $F^L$ ,  $F^T$  and  $F^B$ ) to be equal to those used in the ghost fluid algorithm update. This definition generally leads to multi-valued fluxes in the region near the interface, e.g.  $F_{i,j}^R \neq F_{i+1,j}^L$ . We measure the conservation errors from two sources. First, in each cell,  $U^{new}$  will not generally be equal to  $U^{old} - \Delta t \Delta y (F^R - F^L) - \Delta t \Delta x (F^T - F^B)$  and we record the difference between these two quantities as the gain  $G$  in the quantity  $U$ . Then we visit each flux location on the grid and account for gains due to our multi-valued flux definition, e.g. at  $\bar{x}_{i+1/2,j}$ , the gain is equal to  $\Delta t \Delta y (F_{i+1,j}^L - F_i^R)$ . The gain at each flux is partitioned and distributed to the two adjacent cells using a weighting based on the values of  $|U^{new}|$ . The resulting values of  $G$  represent the net conservation errors committed by a cell. Note that  $G$  will be identically zero away from the interface where a standard conservative scheme is used.

Before subtracting the gains from each cell, we first consider locally smoothing the values of  $G$  under the guise of “mass redistribution”.

[10], [7] and [28] propose a number of methods for mass redistribution including mass weighting, volume weighting, and characteristic based schemes. We take a simpler approach to this problem under the observation that our non-conservative update produces nearly adequate results, i.e. our strategy is to perturb the non-conservative update as little as possible. With this in mind, it makes little sense to add gains to one cell and subtract gains from a neighboring cell. Thus, we sweep through the grid to find fluxes across which the sign of  $G$  changes, redistributing the values of  $G$  to make one of these two values identically zero. While this is the only redistribution method we currently apply, we recognize the importance of future work in this area.

The final step consists of subtracting the gains from each cell. First we rescale the gains to point values by dividing by  $\Delta x \Delta y$ . Then we modify both the values of the real fluid and the values of the ghost fluid according to

$$U_1^{n+1} - = G |U_1^{n+1}| / (f |U_1^{n+1}| + (1-f) |U_2^{n+1}|)$$

$$U_2^{n+1} - = G |U_2^{n+1}| / (f |U_1^{n+1}| + (1-f) |U_2^{n+1}|)$$

so that  $(f U_1^{n+1} + (1-f) U_2^{n+1}) \Delta x \Delta y = U^{new} - G$  making the scheme conservative.

We tested this method on a number of problems including both contact discontinuities and shock waves in both one and two spatial dimensions. We monitored the results and note that the scheme is conservative to machine precision (i.e. 13-15 decimal places). For shock waves, the fully conservative ghost fluid method seems to give similar or better results than the original non-conservative method of [16]. For example, in cases where the non-conservative method computes a shock location that is in error by one or two grid cells, the

fully conservative method tends to get the shock location in the correct cell.

Figure 1 shows an example calculation of a Sod shock tube in one spatial dimension using 200 grid cells. Note that the shock is truly discontinuous. Figures 2-4 show the results of a two-dimensional test case where the initial data consisted of a circle of high pressure (and density) gas at rest. 200 grid cells were used in each spatial dimension. Figure 2 depicts the shock, contact, and rarefaction in order from outside to inside. Note that the shock is truly discontinuous. Figure 3 shows the solution at a later time where the profile behind the shock wave is sloped (i.e. not constant as it is in one spatial dimension). Here conservation helps to predict the correct shock speed since the post-shock state can be adversely affected by the sloping profile behind the wave. Figure 4 shows the location of the zero level set (i.e. the shock wave) at various snapshots in time.

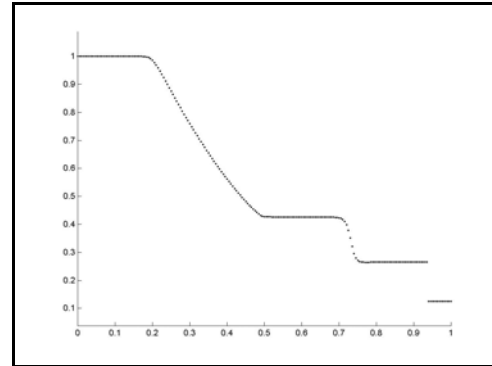


Figure 1: Density profile for the Sod shock tube.

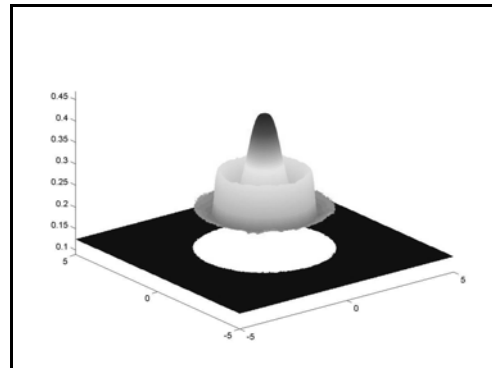


Figure 2: Density profile for a 2D expanding gas.

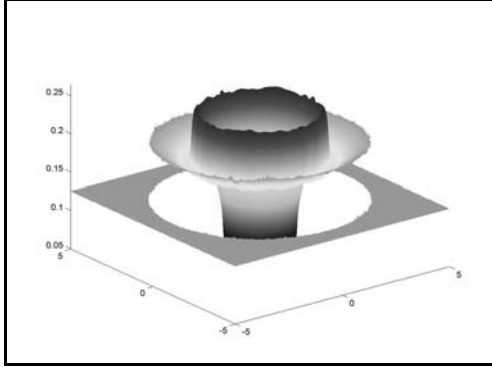


Figure 3: Density profile for a 2D expanding gas.

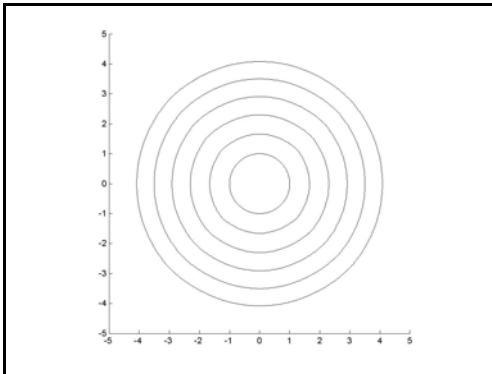


Figure 4: Time snapshots of the shock location.

## 5 - Stiff Detonations Waves

We discretize the reactive Euler equations with a third order accurate ENO-LLF scheme in space and a third order accurate TVD Runge-Kutta scheme in time, see [29]. The level set evolution and reinitialization equations are discretized with a fifth order accurate HJ WENO [24] scheme in space and a third order accurate TVD Runge-Kutta scheme in time. We separate the time integration of the source term from the time integration of the hydrodynamics with Strang splitting [30]. Then we use the backward Euler scheme along with a hybrid bisection/secant root finding method to implicitly integrate the source term.

First consider the simulation of a Chapman-Jouguet detonation wave with  $\gamma = 1.2$ ,  $e_o = 50$ ,  $T_i = 50$  and  $K = 10000$ . The unreacted gas is at

rest with  $\rho = 1$  and  $p = 3$ . See [13] for more details. Figure 5 shows the traveling wave profile computed using 200 grid cells. Note that the leading shock wave is truly discontinuous. The large value of  $K$  makes it difficult to compute valid post-shock states, and thus conservation is important in determining the correct wave speeds. We did not observe any nonphysical one-grid-cell per time step waves in our experiments using either Arrhenius or Heaviside kinetics.

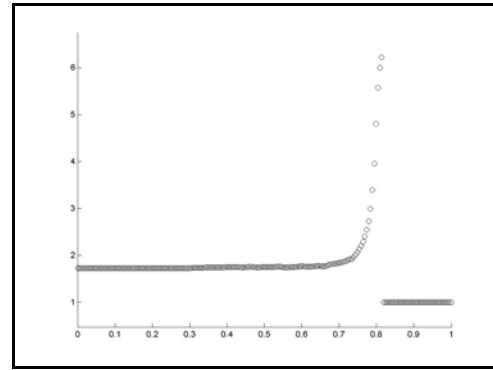


Figure 5: Density profile of a detonation wave.

Should one experience problems in cases where  $K$  is very large, e.g. due to inaccurately calculated post-shock states, our level set based algorithm allows us to easily delay the reaction by a vanishing,  $O(\Delta x)$ , perturbation to the induction time along the lines of [13]. More precisely, we use the level set function to delay the reaction for a few grid cells in the normal direction behind the inert shock, e.g. by starting the reaction only when  $\Phi < -n\Delta x$  (i.e. a delay of  $n$  grid points). This allows us to compute a valid post shock state even for small induction times and stiff chemical reactions.

In two spatial dimensions, we consider a channel of length 3 and width .5 with solid wall boundary conditions on the top and bottom of the domain. The initial data was the same as in our one-dimensional case except that we perturbed the initial condition in a sinusoidal manner. See [13] for more details. Figure 6

shows time snapshots of the zero level set (i.e. shock location) as it moves from left to right. Note the evolution of the triple points. For this example, we used our fully conservative ghost fluid method and a 2 grid point delay of the reaction on a grid with 300x50 grid cells. Figure 7 shows some time snapshots of the density contours.

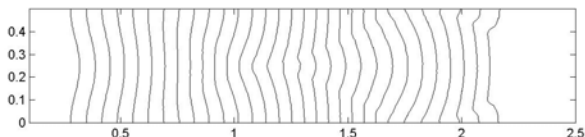


Figure 6: Time snapshots of the shock location.

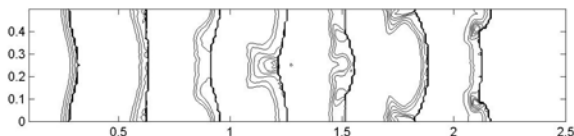


Figure 7: Time snapshots of density contours.

## 6 - Conclusion

We presented a new, fully conservative version of the ghost fluid method applicable for tracking material interfaces, inert shocks, and both deflagration and detonation waves in as many as three spatial dimensions. Future work will address options associated with the “mass redistribution” procedure, e.g. one might consider adjusting the position of the level set to minimize the corrections needed to obtain full conservation (we are currently pursuing this in collaboration with Tariq Aslam, LANL).

## Acknowledgment

Research supported in part by an ONR YIP and PECASE award N00014-01-1-0620. The first and third authors were also supported in part by the DOE ASCI Academic Strategic Alliances Program (LLNL contract B341491). The

second author was also supported in part by a NSF postdoctoral fellowship (DMS-0102029).

The authors would like to express their gratitude to Dr. Wen Masters (ONR) for having faith in this project. They also acknowledge the aid of Bjorn Sjogreen who provided codes to construct the initial data for figures 5, 6 and 7.

## References

- [1] Adalsteinsson, D. and Sethian, J., *The Fast Construction of Extension Velocities in Level Set Methods*, J. Comput. Phys. **148**, 2-22 (1999).
- [2] Aivazis, M., Goddard, W., Meiron, D., Ortiz, M., Pool, J. and Shepherd, J., *A Virtual Test Facility for Simulating the Dynamic Response of Materials*, Computing in Science and Engineering **2**, 42-53 (2002)
- [3] Aslam, T., *A Level Set Algorithm for Tracking Discontinuities in Hyperbolic Conservation Laws*, J. Comput. Phys. **167**, 413-438 (2001).
- [4] Aslam, T., Bdzil, J. and Stewart, D., *Level Set Methods Applied to Modeling Detonation Shock Dynamics*, J. Comput. Phys. **126**, 390-409 (1996).
- [5] Bao, W. and Jin, S., *The Random Projection Method for Hyperbolic Conservation Laws with Stiff Reaction Terms*, J. Comput. Phys. **163**, 216-248 (2000).
- [6] Bao, W. and Jin, S., *The Random Projection Method for Stiff Multispecies Detonation Capturing*, J. Comput. Phys. **178**, 37-57 (2002).
- [7] Bell, J., Colella, P. and Welcome, M., *Conservative Front-Tracking for Inviscid Compressible Flow*, UCRL-JC-105251, LLNL (1991).
- [8] Bihari, B. and Schwendeman, D., *Multiresolution Schemes for the Reactive Euler Equations*, J. Comput. Phys. **154**, 197-230 (1999).
- [9] Caiden, R., Fedkiw, R. and Anderson, C., *A Numerical Method for Two Phase Flow Consisting of Separate Compressible and*

- Incompressible*, J. Comput. Phys. **166**, 1-27 (2001).
- [10] Chern, I.-L. and Colella, P., *A Conservative Front Tracking Method for Hyperbolic Conservation Laws*, UCRL-97200, LLNL (1987).
- [11] Chorin, A., *Random Choice Methods with Applications to Reacting Gas Flow*, J. Comput. Phys. **25**, 253-272 (1977).
- [12] Colella, P., Majda, A. and Roytburd, V., *Theoretical and Numerical Structure for Reacting Shock Waves*, SIAM J. Sci. Comput. **7**, 1059-1080 (1986).
- [13] Engquist, B. and Sjögreen, B., *Robust Difference Approximations of Stiff Inviscid Detonation Waves*, UCLA CAM 91-03 (1991).
- [14] Fedkiw, R., *Coupling an Eulerian Fluid Calculation to a Lagrangian Solid Calculation with the Ghost Fluid Method*, J. Comput. Phys. **175**, 200-224 (2002).
- [15] Fedkiw, R., Aslam, T., Merriman, B. and Osher, S., *A Non-Oscillatory Eulerian Approach to Interfaces in Multimaterial Flows (The Ghost Fluid Method)*, J. Comput. Phys. **152**, 457-492 (1999).
- [16] Fedkiw, R., Aslam, T. and Xu, S., *The Ghost Fluid Method for Deflagration and Detonation Discontinuities*, J. Comput. Phys. **154**, 393-427 (1999).
- [17] Fedkiw, R., Merriman, B. and Osher, S., *Simplified Discretization of Systems of Hyperbolic Conservation Laws Containing Advection Equations*, J. Comput. Phys. **157**, 302-326 (2000).
- [18] Glimm, J., *Solutions in the Large for Nonlinear Hyperbolic Systems of Equations*, Commun. Pure Appl. Math. **18**, 697-715 (1965).
- [19] Glimm, J., Grove, J., Li, X.-L., Oh, W. and Sharp, D., *A Critical Analysis of Rayleigh-Taylor Growth Rates*, J. Comput. Phys. **169**, 652-667 (2001).
- [20] Glimm, J., Grove, J., Li, X.-L. and Zhao, N., *Simple Front Tracking*, Nonlinear Partial Differential Equations, Contemporary Mathematics, edited by Chen, G.-Q. and Di Benedetto, American Mathematical Society **238**, 133-150 (1999).
- [21] Glimm, J., Marchesin, D. and McBrien, O., *Subgrid Resolution of Fluid Discontinuities*, J. Comput. Phys. **37**, 336-354 (1980).
- [22] Glimm, J., Xia, L., Liu, Y. and Zhao, N., *Conservative front tracking and level set algorithms*, PNAS **98**, 14198-14201 (2001).
- [23] Harten, A., *Multiresolution Algorithms for the Numerical Solutions of Hyperbolic Conservation Laws*, Comm. Pure Appl. Math. **48**, 1305-1342 (1995).
- [24] Jiang, G.-S. and Peng, D., *Weighted ENO Schemes for Hamilton Jacobi Equation*, SIAM J. Sci. Comput. **21**, 2126-2143 (2000).
- [25] Lax, P. and Wendroff, B., *Systems of Conservation Laws*, Comm. Pure Appl. Math. **13**, 217-237 (1960).
- [26] Osher, S. and Fedkiw, R., *The Level Set Method and Dynamic Implicit Surfaces*, Springer-Verlag, New York, (2002), in press.
- [27] Osher, S. and Sethian, J., *Fronts Propagating with Curvature Dependent Speed: Algorithms Based on Hamilton-Jacobi Formulations*, J. Comput. Phys. **79**, 12-49 (1988).
- [28] Pember, R., Bell, J., Colella, P., Crutchfield, W. and Welcome, M., *An Adaptive Cartesian Grid Method For Unsteady Compressible Flow in Irregular Regions*, J. Comput. Phys. **120**, 278-304 (1995).
- [29] Shu, C.-W. and Osher, S., *Efficient Implementation of Essentially Non-Oscillatory Shock Capturing Schemes II*, J. Comput. Phys. **83**, 32-78 (1989).
- [30] Strang, G., *On the Construction and Comparison of Difference Schemes*, SIAM J. Numer. Anal. **5**, 506-517 (1968).
- [31] Sussman, M., Smereka, P. and Osher, S., *A Level Set Approach for Computing Solutions to Incompressible Two-Phase Flow*, J. Comput. Phys. **114**, 146-154 (1994).
- [32] Zhang, Y., Yeo, K., Khoo, B. and Wang, C., *3D Jet Impact and Toroidal Bubbles*, J. Comput. Phys. **166**, 336-360 (2001).